# Activity-based protein profiling of diacylglycerol lipases

Baggelaar, M.P.

# CHAPTER 6

# Chemical Proteomics Maps Brain Region Specific Activity of Endocannabinoid Hydrolases*

## Introduction

The endocannabinoid system consists of the cannabinoid type 1 and 2 ($CB_1$ and $CB_2$) receptors, lipid messengers termed endocannabinoids, and the hydrolytic enzymes responsible for the biosynthesis and catabolism of these lipid signaling molecules. 2-Arachidonoylglycerol (2-AG) and anandamide (AEA) are the two main endocannabinoids.[1] The $CB_1$ receptor is highly expressed in the central nervous system, while the $CB_2$ receptor is more abundant in immune cells. The $CB_1$ receptor is among the most abundant G-protein coupled receptors in the brain and modulates a wide variety of signaling events, including inhibition of adenylate cyclase activity, stimulation of ERK activation, closure of voltage-sensitive $Ca^{2+}$ channels and opening of $K^+$ channels.[2,3] Activation of the $CB_1$ receptor is associated with multiple physiological processes, such as energy balance, learning and memory, pain sensation, and neuro-inflammation.[4-7] Unlike classical polar neurotransmitters, which are stored in presynaptic vesicles, 2-AG and AEA are synthesized "on-demand" from post-synaptic membranes and act as retrograde messengers activating presynaptic $CB_1$ receptors, thereby modulating neurotransmitter release. This implies that the biosynthetic and catabolic machinery of the endocannabinoids tightly regulates $CB_1$ receptor activation.[8]

*Baggelaar, M. P.; van Esbroeck, A. C. M.; van Rooden, E.; Florea, B. I.; Overkleeft, H. S.; Marsicano, G.; Chaouloff, F.; van der stelt, M. Chemical Proteomics Maps Brain Region Specific Activity Of Endocannabinoid Hydrolases. *ACS Chem. Biol*. **2017**, DOI: 10.1021/acschembio.6b01052.

Several biosynthetic and catabolic endocannabinoid hydrolases control 2-AG and AEA levels (Figure 1). Diacylglycerol lipase-α and -β (DAGL-α and DAGL-β) are the main enzymes producing 2-AG. They display a tissue specific distribution and studies using mice with congenital deletion of DAGL-α or DAGL-β have identified DAGL-α as the primary enzyme responsible for the biosynthesis of 2-AG in the brain.[9,10] α,β-Hydrolase domain-containing protein 6 and 12 (ABHD6 and ABHD12) and monoacylglycerol lipase (MAGL) inactivate 2-AG by hydrolysis to give arachidonic acid (AA) and glycerol. MAGL is responsible for the bulk hydrolysis of 2-AG, while ABHD6 and ABHD12 play a more distinct role in specific cell populations.[11]

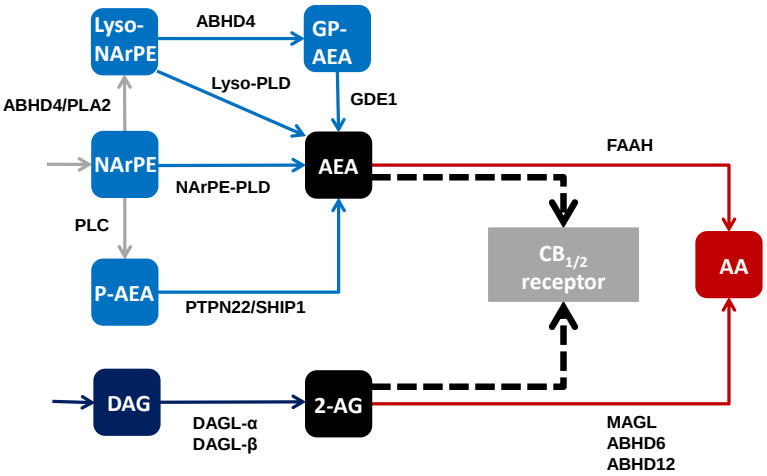


**Figure 1.** Biosynthetic and catabolic pathways of 2-AG and AEA.

The biosynthetic pathways towards AEA appear to be more complex compared with those of 2-AG.[4,6] *N*-arachidonoyl-phosphatidylethanolamine (NArPE) is a key intermediate in AEA biosynthesis. NArPE can be converted via multiple phospholipase-dependent pathways to AEA: (*a*) hydrolysis by *N*-acylphosphatidylethanolamine-phospholipase D (NAPE-PLD), a metallo-β-lactamase, producing AEA and a phosphatidic acid in one step.[12] (*b*) phospholipase $A_2$ ($PLA_2$) and α,β-hydrolase domain-containing protein 4 (ABHD4) mediated conversion to lyso-NArPE, followed by the action of an unknown lysophospholipase D (PLD). Of note, lyso-NArPE can also be converted in a two-step sequence by ABHD4 to glycerophospho-AEA (GP-AEA) and subsequently hydrolyzed to AEA by glycerophosphodiesterase 1 or 4 (GDE1 or GDE4),[13,14] (*c*) in macrophages NArPE serves as a substrate for an unidentified phospholipase C yielding phospho-AEA. Hydrolysis of the phosphate group by phosphatases PTPN22 or SHIP1 provides AEA.[15,16] The enzymatic inactivation of AEA is less complex and is primarily

mediated by fatty acid amide hydrolase (FAAH), which hydrolyses AEA towards arachidonic acid and ethanolamine.[4,17]

Monitoring the activity of the different endocannabinoid hydrolases in various brain regions is key to gain insight in spatiotemporal control of $CB_1$ receptor activation and its physiological role. The existence of a feedback mechanism in anterograde neurotransmitter systems through presynaptic "autoreceptors" to control the release of the neurotransmitters has led to the hypothesis that such an autoregulatory mechanism could also be present in retrograde systems, such as the endocannabinoid system.[18-20] Previous studies have investigated the effect of $CB_1$ receptor modulation on basal endocannabinoid levels. Several studies observed changes in AEA and/or 2-AG levels[21-25], whereas others did not.[18,26] Interestingly, Maccarrone *et al.* found that the endocannabinoid system of $CB_1$ knockout mice adapted with age by upregulating AEA catabolism.[23,24] Recently, Belluomo *et al.* reported that MAGL inhibitor JZL-195 reduced 2-AG accumulation rates in the frontal cortex of mice lacking the $CB_1$ receptor in glutamatergic neurons and an increase of 2-AG accumulation under the same conditions in mice with congenital deletion of the $CB_1$ receptor in astrocytes.[18] In addition, chronic elevation of 2-AG levels by genetic deletion of MAGL or repeated administration of JZL184 led to $CB_1$ receptor desensitization.[27] These observations suggest that there is a crosstalk between the $CB_1$ receptor and the endocannabinoid regulatory machinery. The pre- and postsynaptic autoregulatory mechanisms controlling endocannabinoid levels are, however, poorly understood.

Studying changes in bulk endocannabinoid levels will not reveal which biosynthetic or catabolic pathways are responsible for the regulation of $CB_1$ receptor activity.[18,26] To this end, the activity of each hydrolytic enzyme should be studied. Over the years a brain region and cell type resolved map of the molecular distribution of endocannabinoid hydrolases has been generated by *in situ* hybridization and global proteomics.[28-30] These studies provided a detailed understanding of the molecular composition of the endocannabinoid system in different brain regions at the mRNA and protein level. However, actual enzymatic activity does not always correlate with mRNA and protein levels in specific brain regions due to post-transcriptional and post-translational processes.[31,32] The activity of DAGL-α is, for example, regulated by CaMKII-mediated phosphorylation and MAGL activity can be modulated by sulfenylation of specific cysteines.[33,34] Consequently, it is important to measure actual enzyme activity in the various brain regions.

Conventional enzyme activity assays rely on radiolabeled substrates and LC/MS-based methods.[35] These assays are expensive, time consuming and measure the activity of one enzyme at a time. Others and we have recently applied comparative activity-based protein profiling (ABPP) and chemo-proteomics to measure serine hydrolase activity in complex proteomes.[36-39] ABPP is a technique, which relies on active site directed chemical probes that form a covalent bond with the catalytic nucleophile of targeted enzymes and have a fluorescent or biotin reporter group for visualization and identification,

respectively.[36] Many enzymes regulating brain endocannabinoid levels (i.e. MAGL, DAGL, FAAH, ABHD4, ABHD6 and ABHD12) belong to the serine hydrolase family, therefore they have conserved structural features, which allow for their targeting by specific activity-based probes (ABPs), such as FP-TAMRA and MB064. Here, we have used ABPP to map the relative activity of endocannabinoid hydrolases in different brain regions, such as cerebellum, frontal cortex, hippocampus and striatum. We applied this method to investigate the existence of an autoregulatory feedback mechanism of the $CB_1$ receptor on the endocannabinoid hydrolase activity by comparing the brains of $CB_1$ receptor knockout mice versus wild-type mice.

**Results**

**Gel-based brain region comparison**

Previously, a β-lactone (MB064) and fluorophosphonate (FP-TAMRA) were applied as tools to study the selectivity of DAGL inhibitors LEI104, LEI105 and DH376.[38,40] The use of two ABPs extends the range of enzymes, because the probes have orthogonal warheads and different recognition elements, leading to a different interaction profile. Here, both ABPs were used to map brain region dependent activity of endocannabinoid hydrolases by comparative ABPP. Global assessment of serine hydrolase activity across four different brain regions was performed using a gel-based assay. Membrane and soluble proteomes from mouse cerebellum, frontal cortex, hippocampus or striatum were incubated with the fluorescent ABP MB064 (250 nM) or FP-TAMRA (500 nM), resolved on SDS-PAGE and followed by in-gel fluorescence detection. Coomassie staining was used as protein loading control. Using MB064, 9 intense bands were identified in the membrane fractions of the mouse brain regions, and the identity of endocannabinoid hydrolase bands could be established using reference inhibitors and KO tissue as previously reported.[38,40]

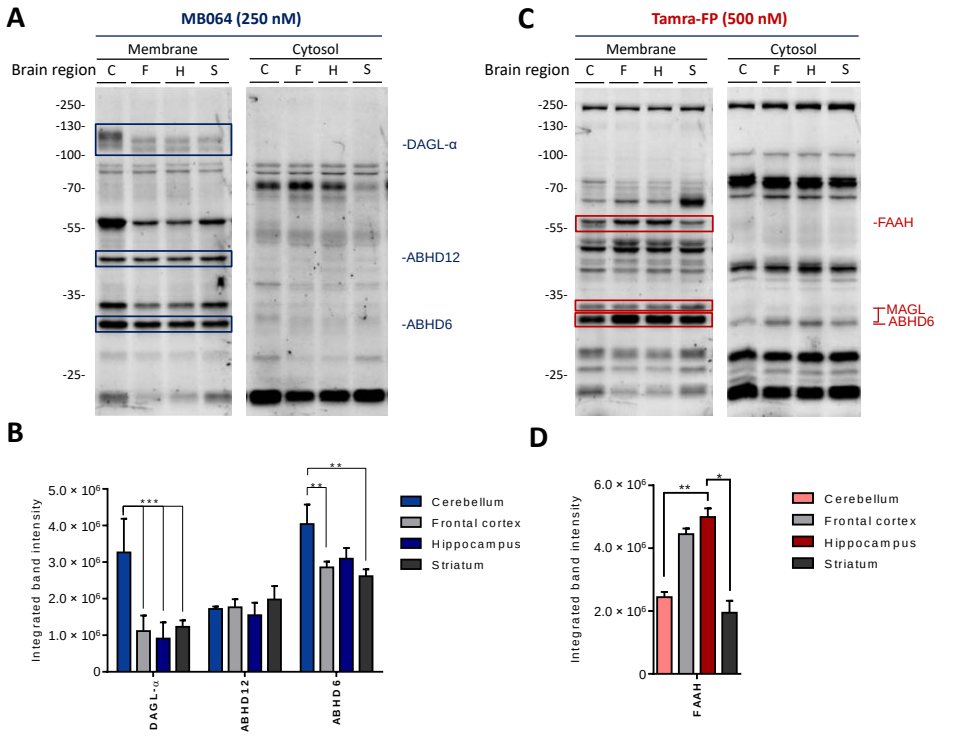


**Figure 2.** Gel based mapping of brain region dependent hydrolase activity. (*A*) Activity-based protein profiling with MB064 in 4 mouse brain regions. (*B*) Quantification of endocannabinoid hydrolase activity as determined with MB064. (*C*) Activity-based protein profiling with FP-TAMRA in 4 mouse brain regions. (*D*) Quantification of FAAH activity as measured with ABP FP-TAMRA. Statistical analysis was performed by means of 2-way ANOVA with Turkey multiple comparisons test (* $P \leq 0.05$; ** $P \leq 0.01$; *** $P \leq 0.001$) (C = cerebellum, F = frontal cortex, H = hippocampus, S = striatum)

In this manner the bands at 120 kDa, 45 kDa and 30 kDa were ascribed to DAGL-α, ABHD12 and ABHD6, respectively. FP-TAMRA labelled FAAH (64 kDa), MAGL (35 and 30 kDa) and ABHD6 (30 kDa). All identified endocannabinoid proteins were present in the four brain regions, but several hydrolases demonstrated pronounced region-dependent activity (Figure 2). For example, DAGL-α activity was ~3 times higher in the cerebellum compared to the frontal cortex, hippocampus and striatum (Figure 2A, B). Interestingly, the fluorescent protein band corresponding to DAGL-α in the cerebellum was shifted towards a higher molecular weight compared to the hippocampus, striatum and frontal cortex. This could indicate that DAGL-α carries a post-translational modification. The activity of ABHD12 was similar in all four brain regions, while the activity of ABHD6 was ~25% higher in the cerebellum compared to the frontal cortex, hippocampus and the striatum. The fluorophosphonate-based ABP revealed the the activity of FAAH to be ~2 times higher in the frontal cortex and the hippocampus. The signals of MAGL and ABHD6 as measured

with this activity-based probe are overlapping and could not be quantified accurately (Figure 2C).

**Chemoproteomic brain region comparison**

To analyze the relative activities in depth, ABPP was coupled to high resolution mass spectrometry. This methodology enables direct identification of the enzymes and provides a more accurate quantification by avoiding band overlap, and yields a broader range of hydrolases due to a higher sensitivity. Membrane and soluble proteomes from cerebellum, hippocampus, frontal cortex or striatum were separately incubated with MB108 or FP-biotin, biotinylated versions of MB064 and FP-TAMRA, respectively. Targeted enzymes were enriched by avidin chromatography, followed by on-bead digest using sequencing grade trypsin. Tryptic peptides from different brain regions were equipped with a different isotopic label by reductive dimethylation with deuterated or non-deuterated formaldehyde. After 1:1 mixing of the differentially labeled brain regions, samples were measured by high resolution MS/MS and analyzed using Maxquant software. (a schematic overview of the chemoproteomic workflow is given in Figure 3a).[41]

Using this chemoproteomic methodology, the relative activity of 34 different hydrolases was quantified in all brain regions, including DAGL-α, FAAH, ABHD12, MAGL, ABHD6 and ABHD4 (See Figure 3 for a heat map). Eleven enzymes reacted with both probes. A high correlation was found between the quantified enzymatic activities for each probe (pearson's correlation of 0.86 ($P < 0.0001$)), indicating probe-independent protein activity was measured (Figure 3). The fluorophosphonate-based ABP targeted 14 unique proteins, including MAGL and FAAH, whereas the β-lactone-based ABP MB108 targeted 7 unique proteins including ABHD4, ABHD12 and DAGL-α. ABHD4 showed an equal activity across all brain regions, while FAAH had the highest activity in the hippocampus and frontal cortex. The activity of DAGL-α in the cerebellum was ~2-fold higher compared to the striatum, hippocampus and frontal cortex. Interestingly, MAGL-activity was lowest in the cerebellum. The results from the chemoproteomic analysis were in line with the gel-based ABPP method, except for ABHD6, which is likely to be caused by band overlap in the gel-based assay. Further detailed analysis showed that overall relative enzymatic activities followed the same trends as observed for the protein abundance derived from a global proteomics data set published by Sharma *et al.* [29] (See supporting figure 1).

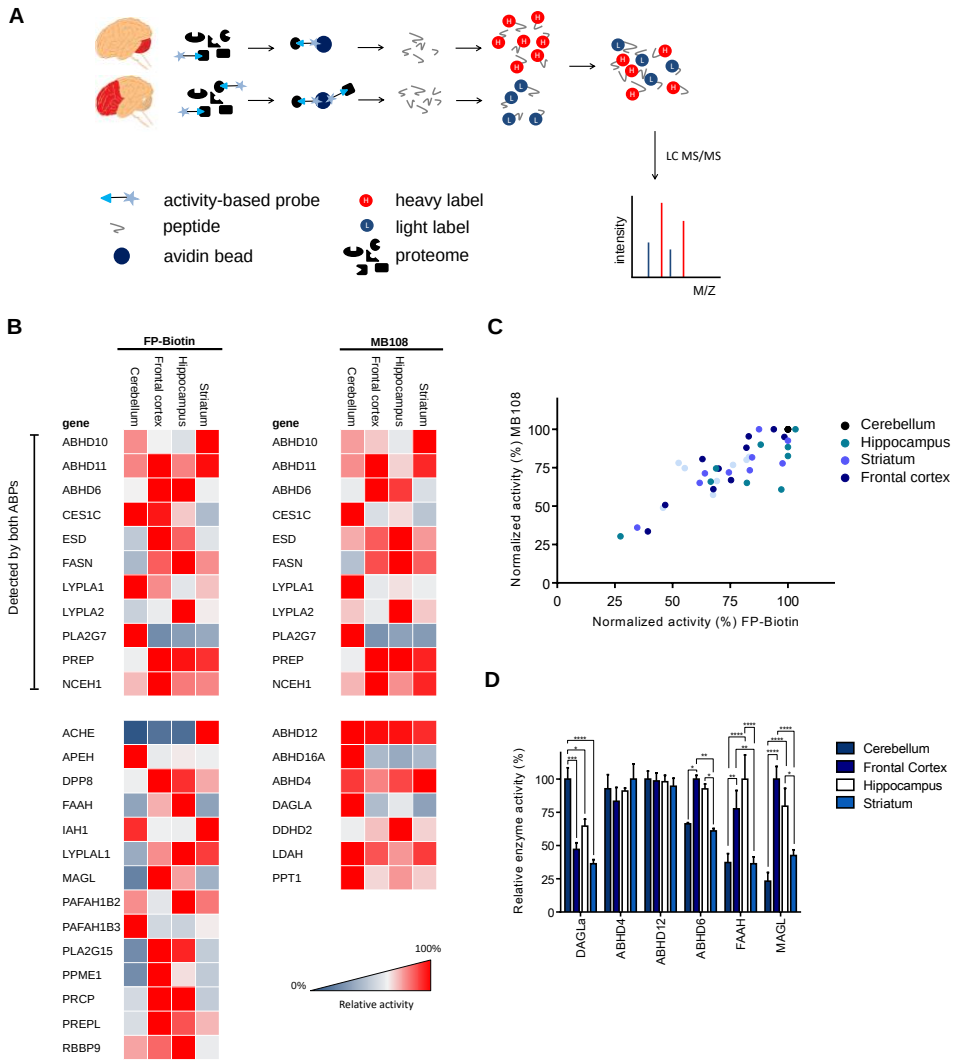


**Figure 3.** Brain region dependent chemoproteomic mapping of relative hydrolase activity. (*A*) Schematic representation of the chemoproteomic workflow. (*B*) Heat map of relative enzyme activity as measured by a fluorophosphonate (FP) based activity-based probe conjugated to a biotin reporter tag (FP-biotin) and a β-lactone based activity-based probe conjugated to a biotin reporter tag (MB108). Data is calculated from the mean ratios of the comparison between cerebellum and striatum, frontal cortex and striatum, and cerebellum and hippocampus. Each comparison was performed in 3 biological replicates. The relative enzyme activity in the brain region in which the serine hydrolase displayed highest activity was set to 100%. (*C*) Correlation graph for enzymes detected by both MB108 and FP-biotin. (*D*) Endocannabinoid regulating enzymes show significant difference between the studied brain regions. Statistical analysis was performed by means of 2 way ANOVA with Turkey multiple comparisons test (* $P \leq 0.05$; ** $P \leq 0.01$; *** $P \leq 0.001$) (C = cerebellum, F = frontal cortex, H = hippocampus, S = striatum)

Of note, several pronounced differences were detected. These different intensity profiles for activity and protein abundance may suggest that protein activity is regulated by post-translational modifications. For example, the activity of ABHD12 was equally distributed over the four brain regions, while ABHD12 abundance in the hippocampus was twice as high as in the cerebellum, frontal cortex and striatum. These different profiles might be explained by a down regulation of ABHD12 activity in the hippocampus. DAGL-α activity was highest in the cerebellum, while its relative activity in the frontal cortex was 47.2 ± 8.6 %, 64.6 ± 9.0% in the hippocampus and 36.3 ± 5.4% in the striatum. In contrast, global proteomics data showed the highest abundance of DAGL-α in the hippocampus, while less than 30% was found in the cerebellum, frontal cortex and striatum. To investigate this apparent discrepancy, we have performed a western blot analysis to check the DAGL-α protein levels in the 4 brain regions of our mice. We observed relatively high DAGL-α abundance in the cerebellum (Figure 4), which matched the relative activity as measured with our ABPP method.

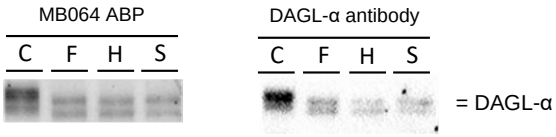


**Figure 4.** Activity based protein profiling and anti DAGL-α western blot in the mouse (C = cerebellum, F = frontal cortex, H = hippocampus, S = striatum)

Many other serine hydrolases were detected next to the endocannabinoid hydrolases (Figure 3). Marked differences in activity between the brain regions were observed for some of these enzymes. For example, acetylcholinesterase (ACHE), which is responsible for acetylcholine hydrolysis, showed over 10-fold activity in the striatum compared to the other three brain regions. ABHD16A, which is a phosphatidylserine lipase producing lyso-phosphatidyl-serine[42], demonstrated a ~2-fold increased activity in the cerebellum compared to other brain regions. Platelet-activating factor acetylhydrolase (PLA2G7), which cleaves the *sn*-2 acetyl of acetyl-glyceryl-ether-phosphorylcholine, showed an approximate 3-fold higher activity in the cerebellum compared to the other brain regions.[43]

**Comparison of $CB_1^{+/+}$ and $CB_1^{-/-}$ brain regions**

Next, the regulatory control of the $CB_1$ receptor over basal production and degradation of endocannabinoids was investigated. To this end, the enzymatic activity of hydrolases involved in endocannabinoid biosynthesis and degradation in the cerebellum, hippocampus, frontal cortex and striatum of $CB_1$ receptor knockout mice was compared to their wild-type counterparts. Fluorescent scanning of gels from ABPP experiments using MB064 and FP-TAMRA did not reveal any difference in labeling patterns in the brain regions (Figure 5).

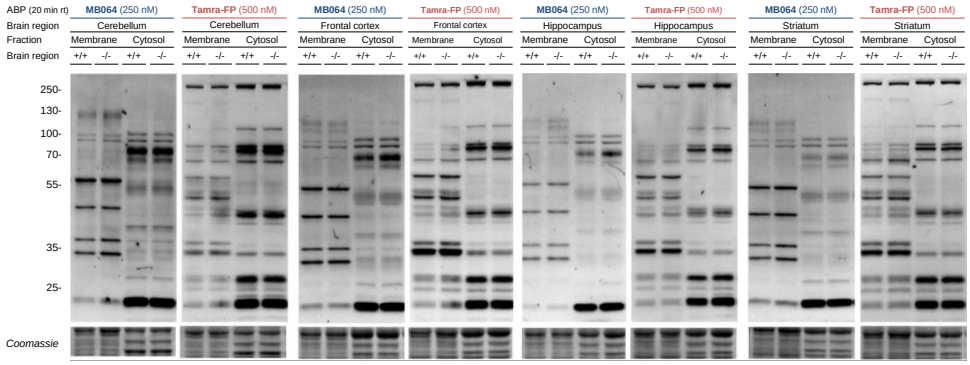


**Figure 5.** Gel based $CB1^{+/+}$ vs $CB1^{-/-}$ comparison. Study of enzyme activity in $CB1^{+/+}$ and $CB1^{-/-}$ mouse brain regions as measured by two activity based probes (MB064 and TAMRA-FP). No difference in enzyme activity between $CB1^{-/-}$ and $CB1^{+/+}$ was observed.

To investigate in depth the effect of $CB_1$ receptor deletion on serine hydrolase activity, the chemo-proteomic assay in the four mouse brain regions was performed. The relative activities of 36 different serine hydrolases were detected and quantified. No difference in the enzymatic activity of the 2-AG biosynthetic enzyme (DAGL-α) and the 2-AG catabolic enzymes ABHD6, ABHD12 and MAGL were observed in the cerebellum, frontal cortex, hippocampus or striatum. Nor were any changes observed in ABHD4 and FAAH activities.

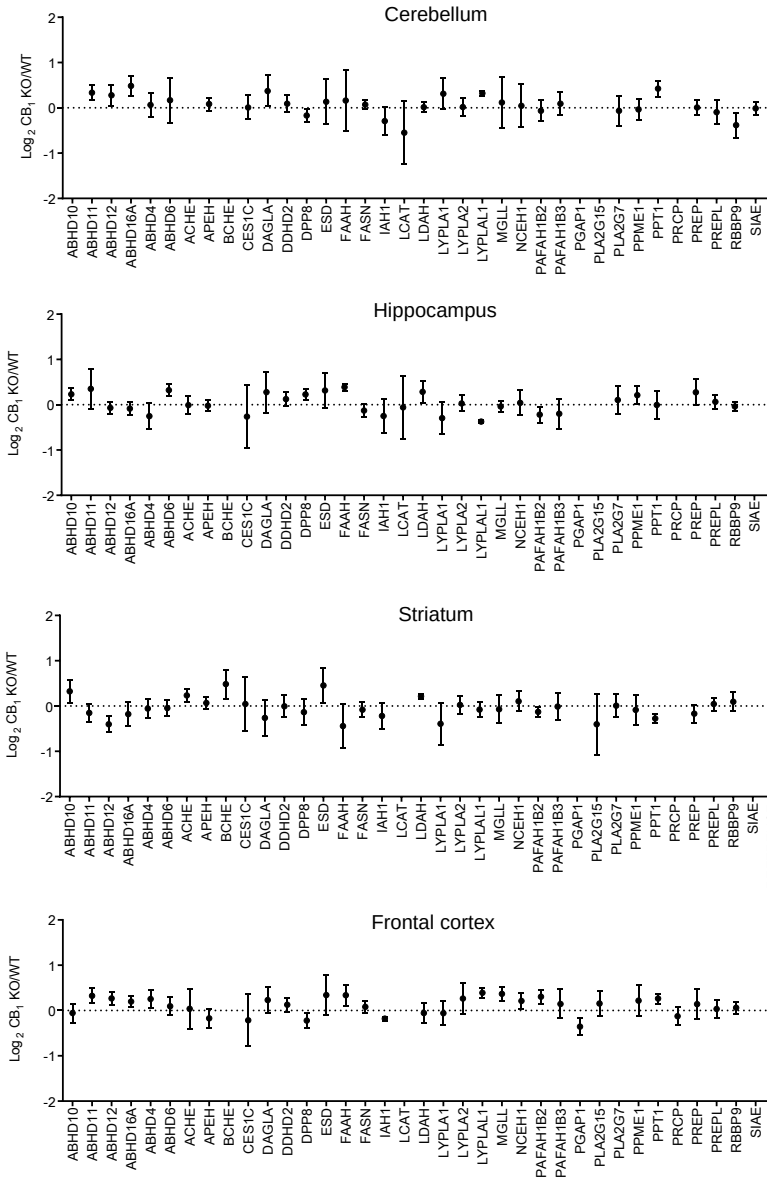


**Figure 6.** Comparison of enzyme activity in $CB1^{+/+}$ and $CB1^{-/-}$ mouse brain regions. $Log_2$ ratio of enzyme activity in $CB1^{-/-}$ brain regions compared to $CB1^{+/+}$. Activity is measured by activity-based proteomics using FP-biotin (10 µM) and MB108 (10 µM). Combined data from both activity based probes (n = 4 for each brain region). Statistical analysis by means of one-way ANOVA, each CB1 WT/KO ratio was compared to a $Log_2$ ratio of 0, subsequently the p values were subjected to Benjamini Hochberg correction. Setting the false discovery rate at 10%.

## Discussion

The enzymes responsible for endocannabinoid biosynthesis and degradation tightly regulate cannabinoid $CB_1$ receptor activation. In this Chapter, a fluorescence and chemoproteomic assay were employed to quantify the activity of hydrolases in the cerebellum, hippocampus, striatum and frontal cortex to gain more insight in the spatiotemporal control of $CB_1$ receptor-mediated physiology. The gel-based fluorescence assay has relatively short experiment time (~3h) and has the ability to retrieve information on differences in protein migration on SDS-PAGE caused by e.g. phosphorylation, glycosylation or proteolysis. Chemoproteomic methodology is complementary and directly reports on the identity and activity of a large number of enzymes in parallel in their native environment with all post-translational modifications in place.

Previous studies have indicated the importance of analyzing different brain regions when studying the endocannabinoid system. Endocannabinoid levels have been shown to vary between brain regions. Moreover, the $CB_1$ receptor and the endocannabinoid regulatory machinery do not present a homogenous expression across brain regions.[1,26,29,44] These variations are confirmed in the comparative ABPP approach using cerebellum, hippocampus, frontal cortex and striatum. Significant differences were found in enzyme activity of DAGL-α, MAGL, ABHD6 and FAAH between different brain regions. For instance, highest FAAH activity was observed in the hippocampus, which is in line with previous reports indicating that the hippocampus has the highest FAAH expression levels, highest AEA levels and turnover rate compared to other brain regions.[18,21,26] These observations suggest that AEA has an important physiological role in the hippocampus, such as providing "on demand" $CB_1$ receptor-dependent neuroprotection against excitotoxicity.[45] Next to its role as an endocannabinoid, AEA functions also as an endogenous agonist of the TRPV1 ion channel.[46] It could be envisioned that FAAH, not only terminates $CB_1$ receptor signaling, but also limits TRPV1 signaling by AEA in the hippocampus. In this respect, it would be interesting to investigate whether TRPV1 mediates crosstalk between AEA and 2-AG biosynthesis as was previously observed in the striatum.[47] Of note, FAAH does not only inactivate AEA, but uses a wide range of long chain fatty acid amides as substrates. The physiological role of these endogenous signaling lipids is poorly understood, but the hippocampus would be an excellent brain region to investigate their biological role.

DAGL-α activity was ~2 fold higher in the cerebellum compared to the frontal cortex, striatum and hippocampus. The activity of MAGL in the cerebellum was only 23.3 ± 11% of the total MAGL activity in the frontal cortex. In addition, no relative compensatory activity of ABHD6 and ABHD12 was observed in the cerebellum (Figure 2). Yet, 2-AG levels are not substantially higher in the cerebellum.[21,26,48] This may suggest that 2-AG levels and $CB_1$ receptor activity are controlled by MAGL, rather than by 2-AG

biosynthesis, or that other catabolic pathways, such as oxidative catabolism, could play a role in this brain region.

Comparison of the activity-based proteomics data with protein expression values from literature showed an overall correlation. For several enzymes (e.g. ABHD16A, ABHD10, ABHD12), however, the activity profile did not match protein abundance profile as reported in a global proteomics data set.[29] This may indicate that the activity of these proteins is regulated by post-translational modifications or could result from differences in the protein expression due to variation in age and mouse species analyzed in the various studies (as observed with DAGL-α).

Previous studies have investigated the effect of $CB_1$ receptor modulation by pharmacological or genetic means on endocannabinoid levels.[18,21-26] Here, this question was revisited and the ABPP-methodology was employed to study the effect of genetic deletion of the $CB_1$ receptor on endocannabinoid hydrolase activity in various brain regions. No significant differences in the activity of endocannabinoid biosynthetic and catabolic enzymes between $CB_1$ KO and WT brain regions were observed. These results are in line with previous reports.[26,18] Yet, it cannot be excluded that specific $CB_1$ receptor populations might increase production and/or degradation whilst others might decrease it, leading to a lack of change when removing all these receptor populations. In support of this hypothesis is the observation that within the frontal cortex the turnover of 2-AG is decreased and increased in mutant mice lacking $CB_1$ receptors on principal neurons (possibly glutamatergic) and on astrocytes, respectively.[18]

Although the proteomics assay is capable to detect a wide array of hydrolases that play an important role in regulation of endocannabinoid signaling, this methodology is not compatible with enzymes that do not form a covalent intermediate with their substrate, such as the β-metallo-lactamase NAPE-PLD. In addition, other mechanisms that regulate endocannabinoid signaling, such as the putative endocannabinoid transporter proteins and oxidative metabolism of endocannabinoids towards eicosanoids, are not taken into account by the ABPP-method.

In conclusion an ABPP method was employed that can measure the activity of six different enzymes with endocannabinoid hydrolase activity in their native setting in a single experiment without having the need of radioactive substrate assays for each individual enzyme. This methodology was used to map endocannabinoid hydrolase activity in the cerebellum, striatum, frontal cortex and cerebellum. This revealed brain region specific differences in endocannabinoid hydrolase activity. The method was applied to study the effect of genetic deletion of the $CB_1$ receptor in these brain regions. The results indicate that the $CB_1$ does not exert regulatory control over the basal production and degradation of endocannabinoids and that genetic deletion of the $CB_1$ receptor does not induce any compensatory mechanism in endocannabinoid hydrolase activity.

## Experimental Methods

### Animals

The experiments were conducted in strict compliance with European directives and French laws on animal experimentation (authorization number C33 12024 to F.C. from the French Ministry of Agriculture). The experiments were conducted on brains of male CB1 WT and KO mice that were sacrificed at the age of 8-9 weeks. The mice were bred at the NeuroCentre INSERM U862.

*Preparation of mouse tissue proteome*. The mouse brain regions; hippocampus, striatum, cerebellum and frontal cortex were slowly thawed on ice. The thawed mouse brain regions were dounce homogenized in cold (4 $^{o}$C) pH 7.2 lysis buffer A (20 mM HEPES pH 7.2, 2 mM DTT, 1 mM $MgCl_2$, 25 U/mL Benzonase) and incubated for 5 minutes on ice. The suspension was centrifuged (2500 × g, 3 min, 4 $^{o}$C) to remove debris. The supernatant was collected and subjected to ultracentrifugation (100.000 × g, 45 min. 4 $^{o}$C, Beckman Coulter, Type Ti70 rotor). This yielded the membrane fraction as a pellet and the cytosolic fraction in the supernatant. The supernatant was collected and the membrane fraction was suspended in storage buffer (20 mM HEPES pH 7.2, 2 mM DTT). The total protein concentration was determined with Quick Start Bradford assay (Biorad) or Qubit$^{TM}$ protein assay (Invitrogen). Membranes and supernatant fractions were both diluted to a total protein concentration of 0.5 mg/mL and were used directly or flash frozen in liquid nitrogen and stored in aliquots at -80 $^{o}$C until use.

### Activity-based protein profiling

Mouse hippocampus, striatum, cerebellum or frontal cortex (0.5 mg/mL) was incubated with activity-based probe MB064 (250 nM) or TAMRA-FP (500 nM) for 20 min at rt. Laemlli buffer was added to quench the protein activity and the mixture was allowed to stand at rt for 30 min before the the samples were loaded and resolved on SDS PAGE gel (10 % acrylamide). The gels were scanned using a ChemiDoc MP system (Cy3 settings, 605/50 filter) and analyzed using Image lab 4.1. After fluorescent scanning, the gels were stained with a coomassie staining solution. After destaining the gels were scanned and protein loading was quantified using image lab 4.1. Gel fluorescence intensities were corrected for protein abundance (loading control).

### Western blot

Proteins were transferred from gel to a PVDF membrane using a Trans-Blot® Turbo (BioRad). The membrane was treated with a blocking solution (5% milk in TBST) for 1 h. The blot was subsequently incubated with the primary antibody rb-anti-DAGLa (D3G8H) (1:1000 in 5% BSA-TBST, 4C, O/N). After washing the blot was incubated with the secondary antbody gt-anti-rb-HRP (1:5000 in 5% BSA-TBST, RT, 1h)). After washing the

blot was developed in the dark using a 10 mL luminal solution, 100 µL ECL enhancer and 3 µL $H_2O_2$. Chemiluminescence was visualized using a ChemiDoc XRS (BioRad).
Actin was used as a control using the same procedure, but using ms-anti-actin (1:5000 in 5% Milk-TBST, 4C, O/N) as primary antibody and gt-anti-ms-HRP (1:5000 in 5% BSA-TBST, RT, 1h) as secondary antibody.

**Proteomics**

Mouse brain region (250 µL, 0.5 mg/mL) membrane or soluble proteome was incubated with vehicle MB108 (µM) or FP-Biotin (10 µM) for 60 min at rt. Subsequently the labeling reaction was quenched and excess probe was removed by chloroform/methanol precipitation. Precipitated proteome was suspended in 500 µL 6M Urea/25 mM ammonium bicarbonate and allowed to incubate for 15 minutes. 5 µL (1 M DTT) was added and the mixture was heated to 65 $^{o}$C for 15 minutes. The sample was allowed to cool to rt before 40 µL (0.5 M) iodoacetamide was added and the sample was alkylated for 30 minutes in the dark. 140 µL 10% (wt/vol) SDS was added and the proteome was heated for 5 minutes at 65 $^{o}$C. The sample was diluted with 6 mL PBS. 100 µL (50 µL for $NPC^{+/+}$ and $NPC^{-/-}$ mouse brains) of 50% slurry of Avidin-Agarose from egg white (Sigma-Aldrich) was washed with PBS and added to the proteome sample. The beads were incubated with the proteome > 2h.
The beads were isolated by centrifugation and washed with 0.5% (wt/vol) SDS and PBS (3x). The proteins were digested overnight with sequencing grade trypsin (Promega) in 100 µL Pd buffer (100 mM Tris pH 7, 100 mM NaCl, 1 mM CaCl2, 2 % ACN and 500 ng trypin) at 37 $^{o}$C with vigorous shaking. The pH was adjusted with formic acid to pH 3 and the beads were removed. The peptides were isotopically labeled by on stage tip dimethyl labeling.
Brain regions were differently labeled with isotopic dimethyl labeling and combined after labeling to allow comparison.

**On–stage tip dimethyl labeling**

The stage tips were made by inserting $C_{18}$ material in a 200 µL pipet. The stepwise procedure given in the table below was followed for stage tip desalting and dimethyl labeling. The solutions were eluted by centrifugal force and the constitutions of the reagents are given below.

| Step | Solution | Centrifugation speed |
|---|---|---|
| Conditioning | Methanol (50 µL) | 2 min 600g |
| Conditioning | Stage tip solution B (50 µL) | 2 min 600g |
| Conditioning | Stage tip solution A (50 µL) | 2 min 600g |
| Loading | Load samples on stage tips | 2.5 min 800g |
| Washing | Stage tip solution A (100 µL) | 2.5 min 800g |
| Dimethyl labeling | Load 20 µL L or M reagents on stage tip | 5 min 400g |
| | Load 40 µL L or M reagents on stage tip | 5 min 400g |
| | Load 40 µL L or M reagents on stage tip | 5 min 400g |
| | Load 40 µL L or M reagents on stage tip | 5 min 400g |
| | Load 30 µL L or M reagents on stage tip | 5 min 400g |
| Washing | Stage tip solution A (100 µL) | 2.5 min 800g |
| Elution | Stage tip solution B (100 µL) | 2.5 min 800g |

**Stage tip solution A**: Stage tip solution A is 0.5% (vol/vol) FA in $H_2O$. (Freshly prepared solution)
**Stage tip solution B**: Stage tip solution B is 0.5% (vol/vol) FA in 80% (vol/vol) ACN/$H_2O$. (Freshly prepared solution).

Dimethyl labeling reagents

| Light labeling reagent | Final concentration | Volume |
|---|---|---|
| Phosphate buffer (50 mM; pH 7.5) | | 900 µL |
| $CH_2O$ (light) | | 50 µL |
| $NaBH_3CN$ (0.6 M) | 0.03 M | 50 µL |

| Medium labeling reagent | Final concentration | Volume |
|---|---|---|
| Phosphate buffer (50 mM; pH 7.5) | | 900 µL |
| $CD_2O$ (Medium) | | 50 µL |
| $NaBH_3CN$ (0.6 M) | 0.03 M | 50 µL |

After the final elution step, the desired heavy and light samples were combined and concentrated on a speedvac to remove the ACN. The residue was reconstituted in 95:3:0.1 $H_2O$/ACN/FA (vol/vol) before LC/MS analysis.

Tryptic peptides were analyzed on a Surveyor nanoLC system (Thermo) hyphenated to a LTQ-Orbitrap mass spectrometer (Thermo) as previously described.[1] Briefly, emitter, trap

and analytical column (C18, 120 Å) were purchased from Nanoseparations (Nieuwkoop, The Netherlands) and mobile phases (A: 0.1% formic acid/$H_2O$, B: 0.1% formic acid/ACN) were made with ULC/MS grade solvents (Biosolve). General mass spectrometric conditions were: electrospray voltage of 1.8-2.5 kV, no sheath and auxiliary gas flow, capillary voltage 40 V, tube lens voltage 155 V and ion transfer tube temperature 150 °C. Polydimethylcyclosiloxane (m/z = 445.12002) and dioctyl phthalate ions (m/z = 391.28429) from the milieu were used as lock mass. Some 10 µl of the samples was pressure loaded on the trap column for 5 min with a 10 µl/min flow and separated with a gradient of 35 min 5%–30% B, 15 min 30%–60% B, 5 min A at a flow of 300 µl/min split to 250 nl/min by the LTQ divert valve. Full MS scans (300–2000 m/z) acquired at high mass resolution (60,000 at 400 m/z, maximum injection time 1000 ms, AGC 106) in the Orbitrap was followed by three MS/MS fragmentations in the LTQ linear ion trap (AGC 5x103, max inj time 120 ms) from the three most abundant ions. MS/MS settings were: collision gas pressure 1.3 mT, normalized collision energy 35%, ion selection threshold of 750 counts, activation q = 0.25 and activation time 30 ms. Ions of z < 2 or unassigned were not analyzed and fragmented precursor ions were measured twice within 10 s and were dynamically excluded for 60 s. Data analysis was performed using Maxquant with acetylation (protein N term) and oxidation (M) as variable modifications. The false discovery rate was set at 1% and the peptides were screened against mouse proteome (Uniprot). Serine hydrolases that were identified in at least two repetitive experiments and for which at least 2 unique peptides were identified were considered as valid quantifiable hits. The activities of proteins were relatively quantified by setting the protein with highest activity at 100%.

**Statistical analysis for $CB_1^{+/+}$ and $CB_1^{-/-}$ comparison.**

For proteins identified by both probes, the normalized ratios from Maxquant were combined for further analysis. Using GraphPad Prism 7.0 software the binary logarithm of each ratio was compared to 0 with one way ANOVA. The resulting p values were subjected to a Benjamini-Hochberg correction, setting the false discovery rate at 10% (q=0.1). Briefly, the p-values of all quantifiable hits were ordered from lowest to highest, and the Benjamini-Hochberg statistic was calculated as q * (position in the list) divided by the number of tests. Subsequently, the proteins for which the p-value is smaller than the BH statistic are controlled for a FDR of q*10%.

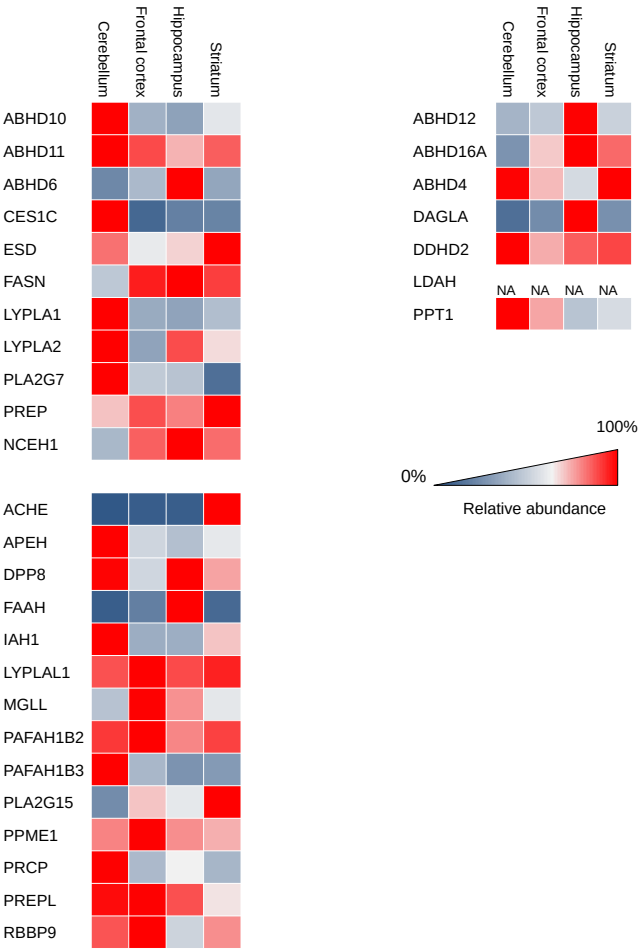


**Supporting Figure 1**. Relative abundance of the hydrolases determined with untargeted proteomics, retrieved from literature.[29]

**References**


1. Mechoulam, R.; Parker, L. A. *Annu. Rev. Physiol.* **2013**, *64*, 21.
2. Dalton, G. D.; Howlett, A. C. *Br. J. Pharmacol.* **2012**, *165*, 2497.
3. Howlett, A. C.; Barth, F.; Bonner, T. I.; Cabral, G.; Casellas, P.; Devane, W. A.; Felder, C. C.; Herkenham, M.; Mackie, K.; Martin, B. R.; Mechoulam, R.; Pertwee, R. G. *Pharmacol. Rev.* **2002**, *54*, 161.
4. Ahn, K.; McKinney, M. K.; Cravatt, B. F. *Chem. Rev.* **2008**, *108*, 1687.
5. Di Marzo, V. *Nat. Neurosci.* **2011**, *14*, 9.
6. Piomelli, D. *Neuropharmacol.* **2014**, *76 Pt B*, 228.
7. Pacher, P.; Batkai, S.; Kunos, G. *Pharmacol. Rev.* **2006**, *58*, 389.
8. Di Marzo, V.; Bifulco, M.; De Petrocellis, L. *Nat. Rev. Drug Discov.* **2004**, *3*, 771.
9. Gao, Y.; Vasilyev, D. V.; Goncalves, M. B.; Howell, F. V.; Hobbs, C.; Reisenberg, M.; Shen, R.; Zhang, M. Y.; Strassle, B. W.; Lu, P.; Mark, L.; Piesla, M. J.; Deng, K.; Kouranova, E. V.; Ring, R. H.; Whiteside, G. T.; Bates, B.; Walsh, F. S.; Williams, G.; Pangalos, M. N.; Samad, T. A.; Doherty, P. *J. Neurosci.* **2010**, *30*, 2017.
10. Tanimura, A.; Yamazaki, M.; Hashimotodani, Y.; Uchigashima, M.; Kawata, S.; Abe, M.; Kita, Y.; Hashimoto, K.; Shimizu, T.; Watanabe, M.; Sakimura, K.; Kano, M. *Neuron* **2010**, *65*, 320.
11. Murataeva, N.; Straiker, A.; Mackie, K. *Br. J. Pharmacol.* **2014**, *171*, 1379.
12. Di Marzo, V.; Fontana, A.; Cadas, H.; Schinelli, S.; Cimino, G.; Schwartz, J. C.; Piomelli, D. *Nature* **1994**, *372*, 686.
13. Sun, Y. X.; Tsuboi, K.; Okamoto, Y.; Tonai, T.; Murakami, M.; Kudo, I.; Ueda, N. *Biochem. J.* **2004**, *380*, 749.
14. Tsuboi, K.; Okamoto, Y.; Rahman, I. A.; Uyama, T.; Inoue, T.; Tokumura, A.; Ueda, N. *Biochim. Biophys. Acta* **2015**, *1851*, 537.
15. Liu, J.; Wang, L.; Harvey-White, J.; Huang, B. X.; Kim, H. Y.; Luquet, S.; Palmiter, R. D.; Krystal, G.; Rai, R.; Mahadevan, A.; Razdan, R. K.; Kunos, G. *Neuropharmacol.* **2008**, *54*, 1.
16. Rahman, I. A. S.; Tsuboi, K.; Uyama, T.; Ueda, N. *Pharmacol. Res.* **2014**, *86*, 1.
17. Cravatt, B. F.; Giang, D. K.; Mayfield, S. P.; Boger, D. L.; Lerner, R. A.; Gilula, N. B. *Nature* **1996**, *384*, 83.
18. Belluomo, I.; Matias, I.; Pernegre, C.; Marsicano, G.; Chaouloff, F. *J. Neurochem.* **2015**, *133*, 26.
19. Starke, K.; Gothert, M.; Kilbinger, H. *Physiological reviews* 1989, *69*, 864.
20. Langer, S. Z. *Trends Pharmacol. Sci.* **1997**, *18*, 95.
21. Di Marzo, V.; Breivogel, C. S.; Tao, Q.; Bridgen, D. T.; Razdan, R. K.; Zimmer, A. M.; Zimmer, A.; Martin, B. R. *J. Neurochem.* **2000**, *75*, 2434.

22. Di Marzo, V.; Berrendero, F.; Bisogno, T.; Gonzalez, S.; Cavaliere, P.; Romero, J.; Cebeira, M.; Ramos, J. A.; Fernandez-Ruiz, J. J. *J. Neurochem.* **2000**, *74*, 1627.
23. Maccarrone, M.; Attina, M.; Bari, M.; Cartoni, A.; Ledent, C.; Finazzi-Agro, A. *J. Neurochem.* **2001**, *78*, 339.
24. Maccarrone, M.; Valverde, O.; Barbaccia, M. L.; Castane, A.; Maldonado, R.; Ledent, C.; Parmentier, M.; Finazzi-Agro, A. *Eur. J. Neurosci.* **2002**, *15*, 1178.
25. Bequet, F.; Uzabiaga, F.; Desbazeille, M.; Ludwiczak, P.; Maftouh, M.; Picard, C.; Scatton, B.; Le Fur, G. *Eur. J. Neurosci.* **2007**, *26*, 3458.
26. Leishman, E.; Cornett, B.; Spork, K.; Straiker, A.; Mackie, K.; Bradshaw, H. B. *Pharmacological Research* **2016**.
27. Schlosburg, J. E.; Blankman, J. L.; Long, J. Z.; Nomura, D. K.; Pan, B.; Kinsey, S. G.; Nguyen, P. T.; H.; Cravatt, B. F. *Nat. Neurosci.* **2010**, *13*, 1113.
28. Kang, H. J.; Kawasawa, Y. I.; Cheng, F.; Zhu, Y.; Xu, X. M.; Li, M. F.; Sousa, A. M. M.; Pletikos, M.; Meyer, K. A.; Sedmak, G.; Guennel, T.; Shin, Y.; Johnson, M. B.; Krsnik, Z.; Mayer, S.; Fertuzinhos, S.; Umlauf, S.; Lisgo, S. N.; Vortmeyer, A.; Weinberger, D. R.; Mane, S.; Hyde, T. M.; Huttner, A.; Reimers, M.; Kleinman, J. E.; Sestan, N. *Nature* 2011, *478*, 483.
29. Sharma, K.; Schmitt, S.; Bergner, C. G.; Tyanova, S.; Kannaiyan, N.; Manrique-Hoyos, N.; Kongi, K.; Cantuti, L.; Hanisch, U. K.; Philips, M. A.; Rossner, M. J.; Mann, M.; Simons, M. *Nat. Neurosci.* **2015**, *18*, 1819.
30. Lein, E. S.; Hawrylycz, M. J.; Ao, N.; Ayres, M.; Bensinger, A.; Bernard, A.; Boe, A. F.; Boguski, M. S.; Brockway, K. S.; Byrnes, E. J.; Chen, L.; Chen, L.; Chen, T. M.; Chin, M. C.; Chong, J.; Crook, B. E.; Czaplinska, A.; Dang, C. N.; Datta, S.; Dee, N. R.; Desaki, A. L.; Desta, T.; Diep, E.; Dolbeare, T. A.; Donelan, M. J.; Dong, H. W.; Dougherty, J. G.; Duncan, B. J.; Ebbert, A. J.; Eichele, G.; Estin, L. K.; Faber, C.; Facer, B. A.; Fields, R.; Fischer, S. R.; Fliss, T. P.; Frensley, C.; Gates, S. N.; Glattfelder, K. J.; Halverson, K. R.; Hart, M. R.; Hohmann, J. G.; Howell, M. P.; Jeung, D. P.; Johnson, R. A.; Karr, P. T.; Kawal, R.; Kidney, J. M.; Knapik, R. H.; Kuan, C. L.; Lake, J. H.; Laramee, A. R.; Larsen, K. D.; Lau, C.; Lemon, T. A.; Liang, A. J.; Liu, Y.; Luong, L. T.; Michaels, J.; Morgan, J. J.; Morgan, R. J.; Mortrud, M. T.; Mosqueda, N. F.; Ng, L. L.; Ng, R.; Orta, G. J.; Overly, C. C.; Pak, T. H.; Parry, S. E.; Pathak, S. D.; Pearson, O. C.; Puchalski, R. B.; Riley, Z. L.; Rockett, H. R.; Rowland, S. A.; Royall, J. J.; Ruiz, M. J.; Sarno, N. R.; Schaffnit, K.; Shapovalova, N. V.; Sivisay, T.; Slaughterbeck, C. R.; Smith, S. C.; Smith, K. A.; Smith, B. I.; Sodt, A. J.; Stewart, N. N.; Stumpf, K. R.; Sunkin, S. M.; Sutram, M.; Tam, A.; Teemer, C. D.; Thaller, C.; Thompson, C. L.; Varnam, L. R.; Visel, A.; Whitlock, R. M.; Wohnoutka, P. E.; Wolkey, C. K.; Wong, V. Y. *Nature* **2007**, *445*, 168.
31. Vogel, C.; Marcotte, E. M. *Nat. Rev. Genet.* **2012**, *13*, 227.
32. Kobe, B.; Kemp, B. E. *Nature* **1999**, *402*, 373.

33. Dotsey, E. Y.; Jung, K. M.; Basit, A.; Wei, D.; Daglian, J.; Vacondio, F.; Armirotti, A.; Mor, M.; Piomelli, D. *Chem. Biol.* **2015**, *22*, 619.
34. Shonesy, B. C.; Wang, X.; Rose, K. L.; Ramikie, T. S.; Cavener, V. S.; Rentz, T.; Baucum, A. J., 2nd; Jalan-Sakrikar, N.; Mackie, K.; Winder, D. G.; Patel, S.; Colbran, R. J. *Nat. Neurosci.* **2013**, *16*, 456.
35. Bisogno, T.; Howell, F.; Williams, G.; Minassi, A.; Cascio, M. G.; Ligresti, A.; Matias, I.; Schiano-Moriello, A.; Paul, P.; Williams, E. J.; Gangadharan, U.; Hobbs, C.; Di Marzo, V.; Doherty, P. *J. Cell Biol.* **2003**, *163*, 463.
36. Cravatt, B. F.; Wright, A. T.; Kozarich, J. W. *Annu. Rev. Biochem.* **2008**, *77*, 383.
37. Niphakis, M. J.; Cravatt, B. F. *Annu. Rev. Biochem.* **2014**, *83*, 341.
38. Baggelaar, M. P.; Chameau, P. J.; Kantae, V.; Hummel, J.; Hsu, K. L.; Janssen, F.; van der Wel, T.; Soethoudt, M.; Deng, H.; den Dulk, H.; Allara, M.; Florea, B. I.; Di Marzo, V.; Wadman, W. J.; Kruse, C. G.; Overkleeft, H. S.; Hankemeier, T.; Werkman, T. R.; Cravatt, B. F.; van der Stelt, M. *J. Am. Chem. Soc.* **2015**, *137*, 8851.
39. Liu, Y.; Patricelli, M. P.; Cravatt, B. F. *Proc. Natl. Acad. Sci. U. S. A.* **1999**, *96*, 14694.
40. Baggelaar, M. P.; Janssen, F. J.; van Esbroeck, A. C.; den Dulk, H.; Allara, M.; Hoogendoorn, S.; McGuire, R.; Florea, B. I.; Meeuwenoord, N.; van den Elst, H.; van der Marel, G. A.; Brouwer, J.; Di Marzo, V.; Overkleeft, H. S.; van der Stelt, M. *Angew. Chem. Int. Ed.* **2013**, *52*, 12081.
41. Cox, J.; Mann, M. *Nat. Biotechnol.* **2008**, *26*, 1367.
42. Kamat, S. S.; Camara, K.; Parsons, W. H.; Chen, D. H.; Dix, M. M.; Bird, T. D.; Howell, A. R.; Cravatt, B. F. *Nat. Chem. Biol.* **2015**, *11*, 164.
43. Long, J. Z.; Cravatt, B. F. *Chem. Rev.* **2011**, *111*, 6022.
44. Herkenham, M.; Lynn, A. B.; Little, M. D.; Johnson, M. R.; Melvin, L. S.; de Costa, B. R.; Rice, K. C. *Proc. Natl. Acad. Sci. U. S. A.* **1990**, *87*, 1932.
45. Marsicano, G.; Goodenough, S.; Monory, K.; Hermann, H.; Eder, M.; Cannich, A.; Azad, S. C.; Cascio, M. G.; Gutierrez, S. O.; van der Stelt, M.; Lopez-Rodriguez, M. L.; Casanova, E.; Schutz, G.; Zieglgansberger, W.; Di Marzo, V.; Behl, C.; Lutz, B. *Science* **2003**, *302*, 84.
46. van der Stelt, M.; Trevisani, M.; Vellani, V.; De Petrocellis, L.; Schiano Moriello, A.; Campi, B.; McNaughton, P.; Geppetti, P.; Di Marzo, V. *EMBO J.* **2005**, *24*, 3026.
47. Maccarrone, M.; Rossi, S.; Bari, M.; De Chiara, V.; Fezza, F.; Musella, A.; Gasperi, V.; Prosperetti, C.; Bernardi, G.; Finazzi-Agro, A.; Cravatt, B. F.; Centonze, D. *Nat. Neurosci.* **2008**, *11*, 152.
48. Buczynski, M. W.; Parsons, L. H. *Br. J. Pharmacol.* **2010**, *160*, 423.